JASMAC Conference of the Japan Society of Microgravity Appllication

P02

Numerical Simulation of Thermal-Solutal Marangoni Convection in a Shallow Rectangular Cavity with Mutually Perpendicular Temperature and Concentration Gradients

Jiangao ZHANG, Atsushi SEKIMOTO, Yasunori OKANO

Department of Materials Engineering Science, Osaka University

1. Introduction

The thermal-solutal Marangoni convection has been widely concerned for its rich dynamical behaviors and its wide existence in nature and industries [1-3]. To the best of our knowledge, most researches only considered the situation of mutually parallel thermal and solutal gradients, and the mutually perpendicular case, which also occurs in some processes, has not been considered. Therefore, in this work, we perform a series of three-dimensional numerical simulations to study thermal-solutal Marangoni convection in a shallow rectangular cavity under the effect of mutually perpendicular thermal and concentration gradients to shed further light on flow characteristics and flow pattern transitions. The present study would be beneficial for a deeper understanding of Marangoni convection and industrial processes such as painting and drying.

2. Numerical method

The fluid motion in a three-dimensional rectangular cavity with a free surface at the top boundary as shown in **Fig. 1** is considered in the Cartesian coordinate system. A high and low temperatures, T_h and T_l, are set at the left and right boundaries, and those for concentration, C_h and C_l are specified at back and front boundaries.

For simplification, we assume that (i) the free surface does not deform; (ii) the fluid is incompressible and Newtonian, and its physical properties do not depend on temperature and concentration except for surface tension; (iii) the no-slip boundary condition is applied except for the top free surface.

By using L, L^2/ν, ν/L as the characteristic length, time, velocity, respectively, the dimensionless governing equations are the conservation of mass, momentum, energy, and mass transfer:

$$\nabla \cdot \mathrm{V} = 0 \tag{1}$$

$$\frac{\partial \mathrm{V}}{\partial \tau} + \mathrm{V} \cdot \nabla \mathrm{V} = -\nabla P + \nabla^2 \mathrm{V} \tag{2}$$

$$\frac{\partial \Theta}{\partial \tau} + \mathrm{V} \cdot \nabla \Theta = -\frac{1}{\mathrm{Pr}} \nabla^2 \Theta \tag{3}$$

$$\frac{\partial \Phi}{\partial \tau} + \mathrm{V} \cdot \nabla \Phi = -\frac{1}{Sc} \nabla^2 \Phi \tag{4}$$

where ν is the kinematic viscosity, the nondimesional temperature and concentrations are defined as $\Theta = (T - T_l)/(T_h - T_l)$ and $\Phi = (C - C_l)/(C_h - C_l)$, τ and P are the dimensionless time and pressure. $Pr = \nu/\alpha$ is the Prandtl number, and $Sc = \nu/D$ is the Schmidt number, where α and D are the thermal diffusivity and the diffusion coefficient of the fluid ($Pr = 0.01$, $Sc = 1$), respectively.

No-slip boundary condition is applied except for top surface, and the boundary condition along free surface are follows:

$$\frac{\partial \mathrm{V}_x}{\partial z} = -Ma_T \frac{\partial \Theta}{\partial x} - Ma_C \frac{\partial \Phi}{\partial x} \tag{4}$$

$$\frac{\partial \mathrm{V}_y}{\partial z} = -Ma_T \frac{\partial \Theta}{\partial y} - Ma_C \frac{\partial \Phi}{\partial y} \tag{5}$$

$$V_z = 0 \tag{6}$$

The thermal and solutal Marangoni numbers are defined as

$$Ma_T = -\sigma_T \frac{(T_h - T_l)L}{\mu \nu}, \quad Ma_C = -\sigma_C \frac{(C_h - C_l)L}{\mu \nu} \tag{7}$$

where $\sigma_T = \partial\sigma/\partial T$ (<0) and $\sigma_C = \partial\sigma/\partial C$ (>0) are the surface tension coefficients of the temperature and concentration fields, respectively. The directions of Marangoni flows are shown in **Fig. 1**.

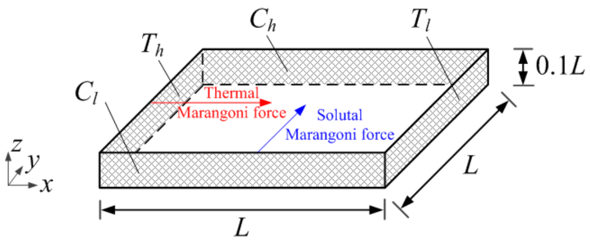

Fig. 1 Numerical computational domain and the boundary conditions. The arrows indicate the directions of each Marangoni convections.

The finite volume method with nonuniform grid is applied to discretize the governing equations and boundary conditions, which are solved by the pressure-implicit split-operator (PISO) algorithm in OpenFOAM. Details of the implementation of the numerical procedure can be found in the work of Minakuchi *et al.* [4]. In addition, the numerical method is validated with the previous result [5] and the mesh dependency is evaluated.

3. Results and discussion

3.1 Basic flow and stability

In the present study, the thermal Marangoni number (Ma_T) is fixed at 0, 1, 3 and 7 $\times 10^4$, the overall Marangoni convection is enhanced by increasing the solutal Marangoni number (Ma_C). When Ma_C is relatively small, the Marangoni convection is the steady flow, which is called as the basic flow. **Figure 2** shows the streamlines, isotherms, and iso-concentration lines of the basic flow as $Ma_C = 5 \times 10^3$. It can be found that the evolution of the basic flow experiences three stages with the increase of the thermal Marangoni number. When $Ma_T = 0$, only the solutal Marangoni convection is applied, the surface fluid flows in the positive y-axis direction by the Marangoni force, then returns back near the bottom due to the mass conservation, as shown in **Fig. 2(a)**. When Ma_T is larger than 0, the thermal and solutal Marangoni forces are perpendicular to each other. As shown in **Fig. 2(b)**, the surface fluid has a tendency to flow in the x-axis. With further increase of thermal Marangoni number, in **Fig. 2(c)**, the fluid basically flows in the x-axis, which means the thermal Marangoni effect is dominant in the whole system.

It is noted that the Lewis number ($Le = Sc/Pr = 100$) in this work is much greater than unity, the heat diffuses much fast than mass. Therefore, the isotherms of the basic flow are almost uniform and parallel to the left and right boundaries, while the iso-concentration lines are much more distorted and sensitive to the flow, as seen in **Fig. 2**.

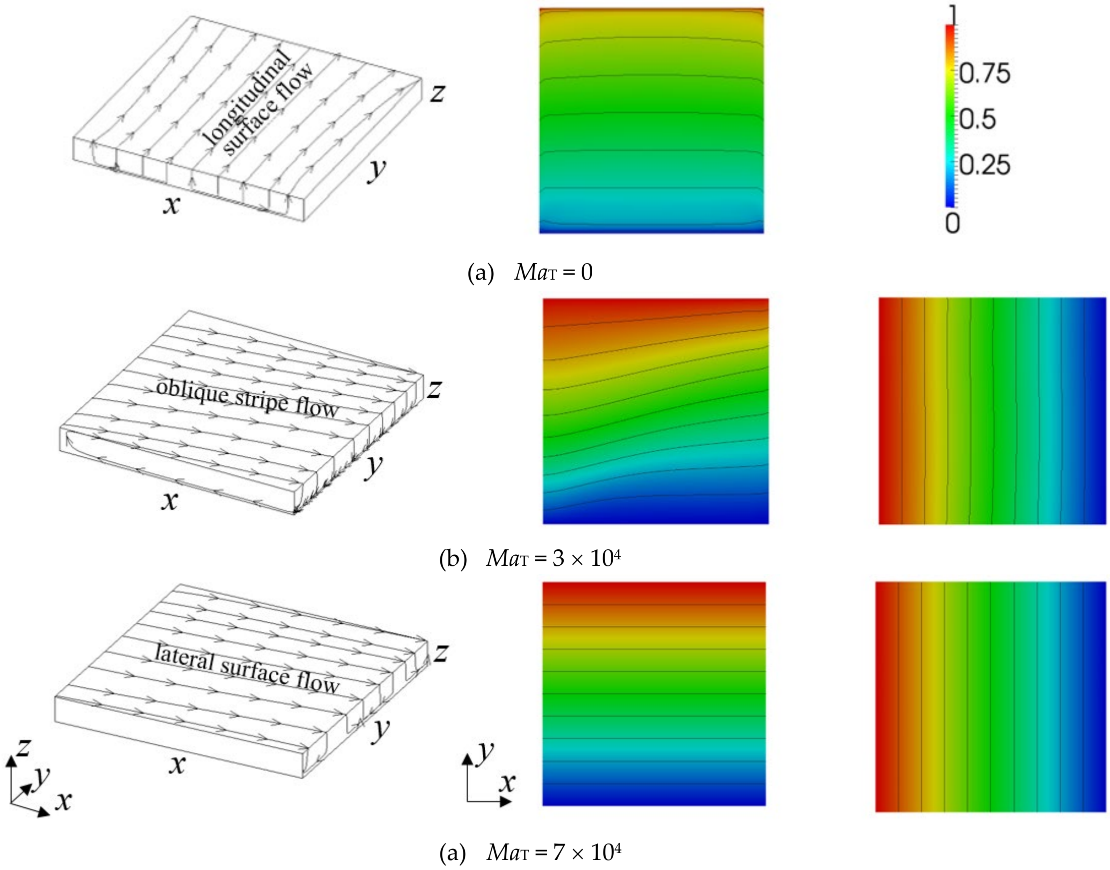

Fig. 2 Streamlines of the boundaries (left), iso-concentration lines (middle) and isotherms (right) on the top free surface as $Ma_C = 5 \times 10^3$. The contour values of temperature and concentration are from 0.1 to 0.9 with steps of 0.1.

3.2 Oscillatory flow

When the solutal Marangoni number exceeds a critical value, the thermal-solutal Marangoni flow bifurcates to an oscillatory flow. **Figure 3** shows the time dependencies of temperature, concentration and longitudinal velocity at the sampling point (A) at $(x, y, z) = (0.5, 0.5, 0.1)$ when $Ma_T = 3 \times 10^4$ and $Ma_C = 3 \times 10^4$. It is clearly shown that the velocity oscillation, V_y, due to the inertial effect of the fluid flow always lags behind the temperature and concentration oscillation, and there is a fixed phase difference among them. Their coupling results in the hydrothermal wave (HTW) and hydrosolutal wave (HSW) instability on the free surface. A similar phase lag between the velocity and temperature oscillations in the HTW or between the velocity and concentration oscillations in HSW was also reported in Refs [6,7].

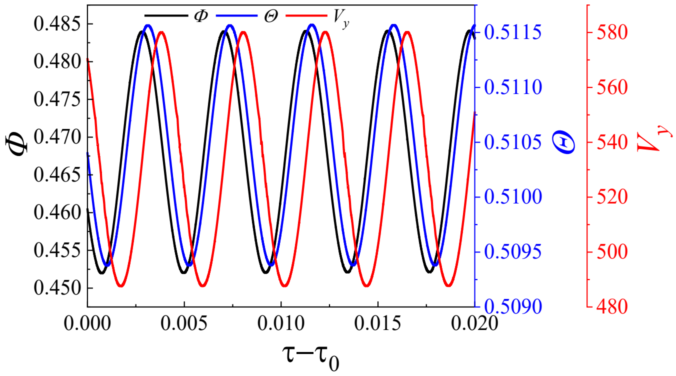

Fig. 3 Time variation of the y- velocity component, temperature, and concentration values at point A at $Ma_T = 3 \times 10^4$ and $Ma_C = 3 \times 10^4$.

4. Conclusion

When the solutal Marangoni number is relatively small, the basic flows can be characterized as three types of steady flow, the longitudinal surface flow, oblique stripe flow, and the lateral surface flow with the increase of the thermal Marangoni number. In addition, the fix phase lag between temperature, concentration, and velocity is observed for oscillatory flow.

Acknowledgements

This work was partially supported by JSPS KAKENHI, Grant No. JP19K22015. The computational resources were provided by the Research Institute for Information Technology, Kyushu University, and Collaborative Research Program for Young Women Scientists provided by Academic Center for Computing and Media Studies, Kyoto University.

References

1) D. Walker and S. DeLong: Contributions to Mineralogy and Petrology, **79** (1982) 231.
2) M. Schmitt and H. Stark: Phys. Fluids, **28** (2016) 012106.
3) D. Kang, A. Nadim, and M. Chugunova: Phys. Fluids, **29** (2017) 072106.
4) H. Minakuchi, Y. Takagi, Y. Okano, K. Mizoguchi, S. Gima, and S. Dost: Journal of Advanced Research in Physics, **3** (2017).
5) J.-M. Zhan, Z.-W. Chen, Y.-S. Li, and Y.-H. Nie: Phys. Rev. E, **82**, (2010) 066305.
6) M. K. Smith: Phys. fluids, **29** (1986) 3182.
7) J.-J. Yu, Y.-R. Li, J.-C. Chen, Y. Zhang, and C.-M. Wu: Int. J. Heat and Mass Transfer, **113** (2017) 40.